XLI CILAMCE
XLI Ibero-Latin American Congress on Computational Methods in Engineering
16-19 November, 2020 FOZ DO IGUAÇU PARANÁ - BRAZIL

Numerical Modelling of Skin Tumor Diagnostics through Dynamic Thermography

Luiz C. Wrobel[1], M. Hriberšek[2], J. Marn[2], J. Iljaž[2]

[1]*Dept. of Civil and Environmental Engineering, Pontifical Catholic University of Rio de Janeiro, PUC-Rio*
Rua Marquês de São Vicente, 225, Gávea, Rio de Janeiro, RJ, CEP 22451-900, Brazil
luiz.wrobel@puc-rio.br
[2]*Faculty of Mechanical Engineering, University of Maribor, Slovenia*
Smetanova ulica 17, Maribor, SI-2000, Slovenia
jurij.iljaz@um.si; matjaz.hribersek@um.si; jure.marn@um.si

Abstract. Dynamic thermography has been clinically proven to be a valuable diagnostic technique for skin tumor detection as well as for other medical applications such as breast cancer diagnostics, diagnostics of vascular diseases, fever screening, dermatological and other applications. Thermography for medical screening can be done in two different ways, observing the temperature response under steady-state conditions (passive or static thermography), and by inducing thermal stresses by cooling or heating the observed tissue and measuring the thermal response during the recovery phase (active or dynamic thermography). Both methods have been used for medical applications; however, recent research on dynamic thermography has shown many advantages over static thermography. The numerical modelling of heat transfer phenomena in biological tissue during dynamic thermography can aid the technique by improving process parameters or by estimating unknown tissue parameters based on measured data. This paper presents a nonlinear numerical model of multilayer skin tissue containing a skin tumor, together with the thermoregulation response of the tissue during the cooling-rewarming processes of dynamic thermography. The model is based on the Pennes bioheat equation and solved numerically by using a subdomain boundary element method which treats the problem as axisymmetric. The paper includes computational tests and numerical results for Clark II and Clark IV tumors, comparing the models using constant and temperature-dependent thermophysical properties, which showed noticeable differences and highlighted the importance of using a local thermoregulation model.

Keywords: boundary element method, dynamic thermography, skin tumor diagnostics

1 Introduction

Thermography or Infrared Thermal (IRT) imaging has become a very valuable tool in recent times due to the development of modern and efficient infrared cameras and related technology, and is mostly used for monitoring in problems where heat transfer plays an important role. IR cameras measure the thermal radiation that is emitted from the observed surface and, based on the intensity and emissivity of the surface, the temperature can be evaluated. Because the method measures the temperature in a contactless manner, it has an advantage over measurement techniques that use temperature sensors that have to be in contact with the material or media under observation. It has therefore found practical use in medicine for various applications such as breast cancer diagnostics, diagnostics of vascular diseases, fever screening, dermatological applications, blood pressure monitoring, etc. [1,2]. In this paper, we will focus on the use of numerical modelling of biological tissues to assist IRT imaging for the early detection of skin tumors, which is very important for the survival rate of patients, especially in the case of malignant melanoma [3-5].

Thermography for medical screening or diagnosis can be done in two ways, observing the temperature under steady-state conditions (passive or static thermography) or inducing thermal stresses by cooling or heating of the

observed tissue and measuring the thermal response during the recovery phase (active or dynamic thermography). Both methods have been used for medical applications: however, recent research on dynamic thermography shows that this is a superior approach over static thermography as it provides more information on the observed tissue [6,7]. Skin tumor has a higher blood perfusion rate and metabolic heat generation than healthy tissue [8], which is reflected in higher temperatures that can be detected by using IRT imaging. However, because of the relative small size of a skin tumor at its early stage, the temperature difference is also small and very difficult to detect using static thermography. Using dynamic thermography with an applied cooling, the temperature difference between the skin tumor and the surrounding healthy tissue during the recovery phase can reach the range of 300mK, which produces a much higher thermal contrast and is easier to observe with an IR camera [9]. Another issue is that the examination time in static thermography can be quite long because of the time needed for the patient to acclimatize to the examination room conditions and to achieve temperature equilibrium [9].

To improve the survival rate of patients with malignant melanoma, the tumor has to be detected at an early stage. The stage of the tumor is usually classified with the Clark level [5]; however, one of the prognosis variable is also the Breslow thickness [10]. Clark et al. [5] classified different skin tumors into levels from I to V, depending on their invasiveness. The Clark I level represents melanoma in situ, which means that the cancerous cells are only in the epidermis, the outer layer of the skin, while Clark V means that it has grown into the fat layer under the skin. Breslow [10] conducted a study on the survival rate of skin melanoma measuring its thickness, diameter and cross-sectional area, and found that if the diameter of the melanoma is less than 5mm there was no metastasis.

This paper presents a new approach for modelling heat transfer in tissue, as it includes the thermoregulation response of the tissue for use in dynamic thermography. The numerical model of skin tumor proposed in this paper describes the thermal response to the external thermal stimulus more realistically, treats the problem as 3D and includes different layers of tissue and temperature-dependent properties or the blood perfusion rate and metabolic heat generation. The model is based on the Pennes bioheat model while the subdomain BEM approach [11] is used to solve the governing equations.

2 Numerical model

The proposed numerical model treats skin tissue as non-homogeneous, composed of several different layers as can be seen in Figure 1, representing the computational domain. The basis for the model was taken from [3,9,12].

The model geometry is cylindrical, with representative diameter and thickness, placed in the center of the computational domain. In this way, the bioheat transfer problem is treated as axisymmetric, which reduces the computational time compared to a full 3D model.

The model shown in Fig. 1 is derived for skin tissue including a tumor. Because there are many uncertainties in the values of some parameters, Iljaz et al. [12] presented a sensitivity analysis of 56 model parameters by using an objective function gradient technique to determine the values of the most important parameters in the model, which are used in this work.

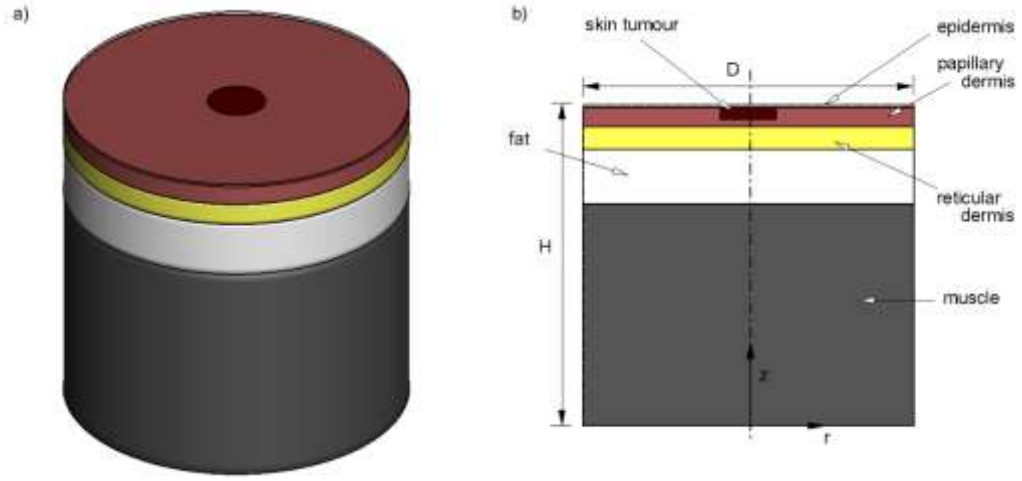

Figure 1. Sketch of the numerical model: a) Isometric view; b) Cross-sectional view

3 Governing equations

The Pennes bioheat model is widely used to describe heat transfer in biological tissue because of its relative simplicity, and is written as follows [13]:

$$\rho\, c\, \partial T/\, \partial t = \nabla.\,(k\nabla T) + \omega_b\, \rho_b\, c_b\, (T_a - T) + q_m \tag{1}$$

where T represents tissue temperature, ρ, c and k are the effective density, specific heat and thermal conductivity of tissue, respectively, ω_b is the blood perfusion rate, ρ_b is blood density, c_b is specific heat of blood, T_a is arterial blood temperature, t is time and q_m is metabolic heat source. The blood perfusion rate is a scalar representing the volumetric blood flow rate per volume of tissue through small arterioles and capillary bed. The blood perfusion acts like a heat source of heat sink inside the tissue, depending on the temperature difference between tissue and arterial blood flow. During the cooling process of dynamic thermography, blood perfusion acts like a heat source, heating up the tissue during thermal recovery, similar to the metabolic heat source which depends on cell activity. Between these two effects, blood perfusion plays a major role in reheating the tissue.

All the parameters in the Pennes equation are usually treated as constant. However, there are many factors that affect the value of these parameters. The parameters are usually estimated or taken from the literature because of the lack of measurement data [3]. It is known that central and local thermoregulation of the human body influence the value of the blood perfusion rate and metabolic heat generation of the skin, muscle and other tissues, which play an important role in keeping the body core temperature constant [14,15]. In other words, thermoregulation tries to keep the human body warm in cold conditions and vice-versa. Therefore, in this paper, a local thermoregulation model that describes blood perfusion rate and metabolic heat generation as temperature-dependent will be adopted. The arterial blood temperature is assumed to be constant and equal to the body core temperature, which is a reasonable assumption because of the application of local cold stress, as well as the fact that the patient is acclimatized during the examination and is a resting position.

The thermoregulation model adopted in this paper uses the van't Hoff Q_{10} effect to model the temperature change of basal metabolic heat generation rate in the tissue. The model developed by Fiala et al. [14] is as follows:

$$q_m = q_{m,bas} + \Delta q_{m,bas} + \Delta q_{m,sh} + \Delta q_{m,w} \tag{2}$$

where $q_{m,bas}$ represents the basal metabolic rate at rest, $\Delta q_{m,bas}$ the change in basal metabolic rate due to temperature change, $\Delta q_{m,sh}$ the shivering effect controlled by the central nervous system, $\Delta q_{m,w}$ the change in metabolic rate due to work or exercise. In the current problem, the shivering and exercise effects are not considered as the patient will be acclimatized and in a resting position. The basal metabolic change due to temperature is modelled by using the van't Hoff Q_{10} effect in the form:

$$\Delta q_{m,bas} = q_{m,bas}\, ({Q_{10,m}}^{(T-T_0)/10} - 1) \tag{3}$$

where $Q_{10,m}$ represents the metabolic rate coefficient that usually takes the value of 2, T is local tissue temperature and T_0 is the body equilibrium temperature. Inserting eq. (3) into eq. (2), the thermoregulation model for metabolic heat generation can be written as

$$q_m(T) = q_{m,bas}\, {Q_{10,m}}^{(T-T_0)/10} \tag{4}$$

A similar model has also been used for the perfusion rate coefficient, as follows:

$$\omega_b\,(T) = \omega_{b,bas}\, {Q_{10,b}}^{(T-T_0)/10} \tag{5}$$

As the bioheat equation is written for each layer or tissue in the model, compatibility and equilibrium conditions have to be imposed along the interface between layers, using a standard BEM sub-regions procedure.

4 Boundary conditions

We now have to prescribe appropriate boundary and initial conditions for the problem. For the bottom part of the domain, we prescribe Dirichlet conditions assuming that the muscle tissue is thick enough to reach the body core temperature, which does not change with time:

$$T(r,z,t) = T_0 \qquad z = 0 \qquad 0 \le r \le D/2 \qquad 0 \le t \le \tau \tag{6}$$

where T_0 represents the body temperature in thermal equilibrium with the surrounding environment, D is the diameter of the computational domain and τ represents the simulation time, including the cooling process.

On the sides of the computational domain, adiabatic boundary conditions are prescribed assuming that the diameter D of the computational domain is sufficiently large not to affect the solution. The boundary condition is of the form

$$\partial T(r,z,t)/\partial r = 0 \qquad 0 \le z \le H \qquad r = D/2 \qquad 0 \le t \le \tau \tag{7}$$

where H is the total height of the computational domain.

For the skin surface, we take into account the cooling process as well as the heat transfer with the surrounding environment during the rewarming phase. A constant cooling approach seems to be the most appropriate because of the deep penetration and high temperature contrast during the rewarming phase. Therefore, the boundary condition is given by

$$T(r,z,t) = T_c \qquad z = H \qquad 0 \le r \le D/2 \qquad 0 \le t \le t_c \tag{8}$$

where T_c represents the cooling temperature and t_c the cooling time. After the cooling time, the skin is exposed to the surrounding environment, which is described by the following Robin condition

$$k\,\partial T(r,z,t)/\partial z = \alpha(T - T_\infty) \qquad z = H \qquad 0 \le r \le D/2 \qquad t_c \le t \le \tau \tag{9}$$

where α represents the heat transfer coefficient, T is the local tissue temperature and T_∞ is the ambient temperature. The heat transfer coefficient can include many effects such as heat convection, thermal radiation and water evaporation [16]. However, thermal radiation is negligible in this case due to the small temperature difference between the skin and the surrounding environment, and does not affect the rewarming process, and so is water evaporation by sweating because the cooling-rewarming process does not induce sweating. The main contribution during rewarming is therefore heat convection with the surrounding environment, that is not intense in this case as the skin rewarms mostly due to the internally generated heat or blood perfusion.

For the initial temperature distribution $T(r,\theta,z,t=0)$, we prescribe the steady-state solution of the bioheat problem determined with boundary conditions (6), (7) and (9).

5 Boundary element method

The subdomain Boundary Element Method (BEM) was used to solve the previously described numerical model. This technique was described in detail in [11] and will not be repeated here. The main points of the current BEM formulation are as follows: the fundamental solution of the axisymmetric Laplace equation is utilized, based on elliptic functions, with the transient and domain terms taken into account by using the subdomain approach as discussed in [12]. A second order finite difference approximation is adopted for the time marching scheme. The elements adopted have quadratic interpolation for the temperature and constant approximation for the heat flux, to avoid the discontinuities of the normal at corners. The cells employed for the domain discretization are also quadratic. The resulting system of equations is non-linear and has to be solved by using an iterative scheme.

6 Computational tests

The computational tests of dynamic thermography for skin tumor were applied for two different tumor sizes, Clark II and Clark IV, showing the differences in thermal response during the rewarming period. For Clark II, the diameter and thickness of the tumor are $d_t = 2$ mm and $h_t = 0.44$ mm, while for Clark IV the equivalent dimensions are $d_t = 2.5$ mm and $h_t = 1.1$ mm. The material properties and tissue dimensions of each layer are as follows [3, 9, 16]:

Epidermis: $h = 0.1$ mm, $\rho = 1200$ kg/m^3, $c_p = 3589$ J/(kg K), k = 0.235 W/(m K)
Papillary dermis: $h = 0.7$ mm, $\rho = 1200$ kg/m^3, $c_p = 3300$ J/(kg K), k = 0.445 W/(m K),
$\omega_{b,bas} = 0.0002$ s^{-1}, $q_{m,bas} = 368.1$ W/m^3
Reticular dermis: $h = 0.8$ mm, $\rho = 1200$ kg/m^3, $c_p = 3300$ J/(kg K), k = 0.445 W/(m K),
$\omega_{b,bas} = 0.0013$ s^{-1}, $q_{m,bas} = 368.1$ W/m^3
Fat: $h = 2$ mm, $\rho = 1000$ kg/m^3, $c_p = 2674$ J/(kg K), k = 0.185 W/(m K),
$\omega_{b,bas} = 0.0001$ s^{-1}, $q_{m,bas} = 368.3$ W/m^3
Muscle: $h = 8$ mm, $\rho = 1085$ kg/m^3, $c_p = 3800$ J/(kg K), k = 0.510 W/(m K),
$\omega_{b,bas} = 0.0027$ s^{-1}, $q_{m,bas} = 684.2$ W/m^3
Clark II tumor: $d = 2$ mm, $h = 0.44$ mm, $\rho = 1030$ kg/m^3, $c_p = 3852$ J/(kg K), k = 0.558 W/(m K),
$\omega_{b,bas} = 0.0063$ s^{-1}, $q_{m,bas} = 3680$ W/m^3
Clark IV tumor: $d = 2.5$ mm, $h = 1.1$ mm, $\rho = 1030$ kg/m^3, $c_p = 3852$ J/(kg K), k = 0.558 W/(m K),
$\omega_{b,bas} = 0.0063$ s^{-1}, $q_{m,bas} = 3680$ W/m^3
Blood: $\rho = 1060$ kg/m^3, $c_p = 3770$ J/(kg K)

The values of the van't Hoff coefficients are taken as $Q_{10,m} = Q_{10,b} = 2$ for all layers with the exception of the tumor, for which $Q_{10,m} = Q_{10,b} = 1.1$, based on values from the literature. The mean body core temperature for a healthy person in a resting position has been set to 37ºC, the same value as for the arterial blood temperature. The ambient temperature was set to 24ºC, and the heat transfer coefficient is equal to 10 W/(m^2 K). The cooling time and cooling temperature are taken as $t_c = 60$ s and T_c =13ºC. We added an extra 10 minutes of simulation time to account for the rewarming period. Therefore, the total simulation time was set to $\tau = 660$ s.

To assure numerical accuracy of the results, mesh and time convergence analysis was performed. The appropriate element size was found to be Δr = 5 mm and the appropriate time step to be Δt = 1s. Figure 2 shows the structured mesh used for the numerical simulations, where the number of elements in the thin layers was a minimum of 2. The domain size adopted in [3, 9, 16] was 12 mm, but we found it appropriate to use a larger domain. For both tumors, the domain size was taken as D = 25 mm.

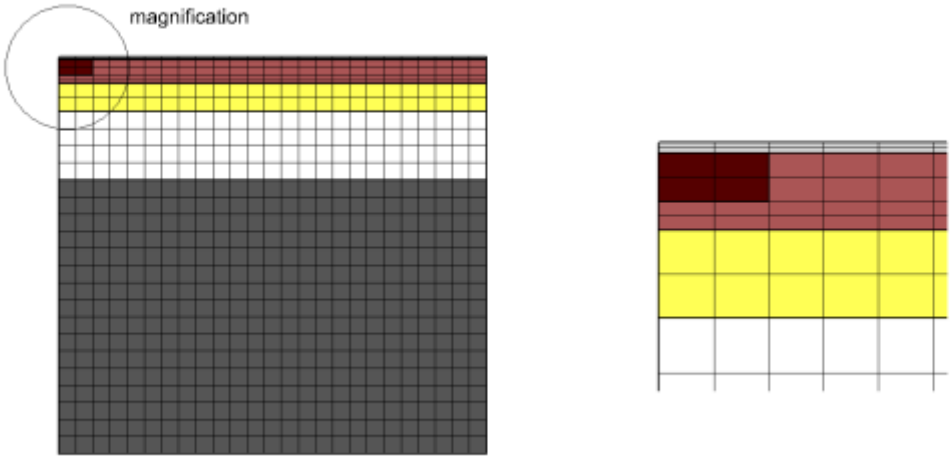

Figure 2. Representative computational mesh for Clark II tumor

The results shown below simulate dynamic thermography for skin tumor screening, showing the temperature response after the cooling period. The most important issue is to get a large temperature difference between the highly vascular skin tumor and the surrounding tissue, to make it possible to detect the tumor in its early stage using an IR camera.

Figure 3 shows the temperature response of the skin tissue and tumor during the rewarming period, where a high temperature difference can be observed, particularly at the beginning of the rewarming period. Figure 3 shows numerical results for Clark II and Clark IV tumors, for constant and time-dependent thermophysical properties. In the first 60 s, the skin is cooled to 13ºC and is then exposed to the environment with a higher temperature of 22.4ºC. Comparing the results obtained with constant and time-dependent thermophysical properties, it can be seen that the model with time-dependent properties predicts a lower peak temperature difference, and also that the difference decreases through time is slightly lower for the model using constant properties, particularly for the Clark IV tumor. However, the temperature differences provoked by the rewarming approach are now high and can be easily detected by an IR camera. As the rewarming period is mostly controlled by the amount of cold applied during the cooling phase, the window time for the rewarming observation can be changed if needed.

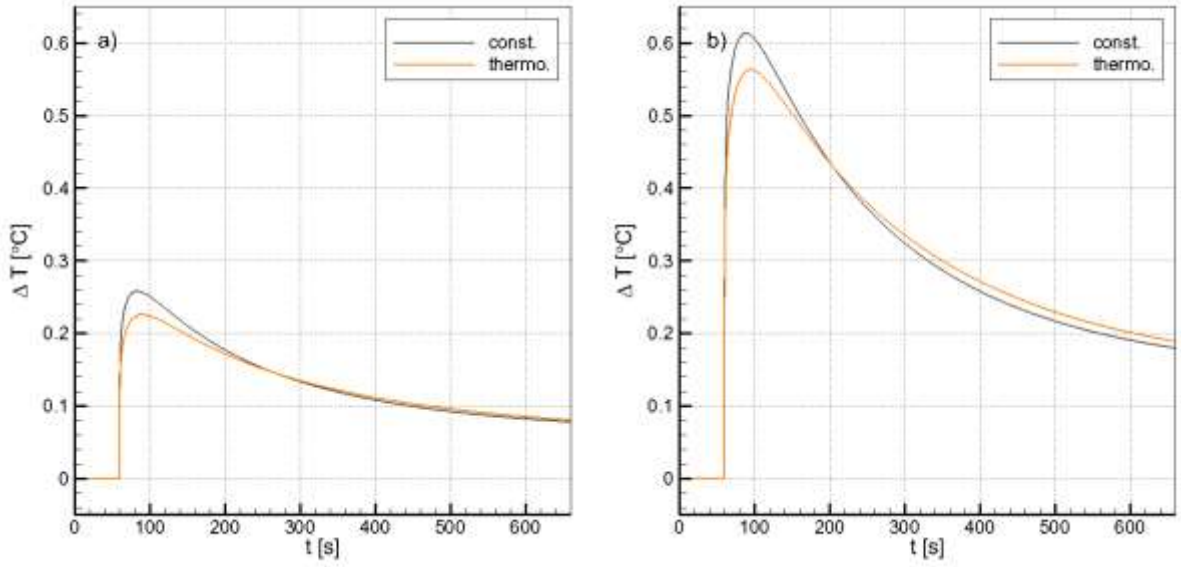

Figure 3. Maximum temperature difference during the rewarming period of dynamic thermography for: a) Clark II; b) Clark IV tumor

7 Conclusions

Dynamic thermography has been shown in many papers to be a promising new non-invasive diagnostic technique not only for the detection of skin tumor but for many other medical applications. The technique involves thermal provokation of the investigated tissue by cooling or heating, and recording its temperature response using an IR camera that reveals much more information about the tissue under consideration than using static thermography. Using this technique, we can also estimate some of the unknown parameters of the problem which are very important for diagnosis or prognosis, based on the temperature response or measurements by solving an inverse problem [17]. For that, we need to use an accurate numerical model that reflects the problem under investigation realistically.

The main novelty of this research is the improved three-dimensional model that includes the thermoregulation response of the cooling-rewarming process, which will contribute to further developments in the field of bioheat modelling or for solving inverse problems in dynamic thermography.

Authorship statement. The authors hereby confirm that they are the sole liable persons responsible for the authorship of this work, and that all material that has been herein included as part of the present paper is either the property (and authorship) of the authors, or has the permission of the owners to be included here.

References

[1] B. Lahiri, S. Bagavathiappan, T. Jayakumar and J. Philip, "Medical applications of infrared thermography: A review". *Infrared Physics & Technology*, vol. 55, n. 4, pp. 221–235, 2012.
[2] C. Magalhães, R. Vardasca and J. Mendes, "Recent use of medical infrared thermography in skin neoplasms". *Skin Research and Technology*, vol. 3, pp. 1–5, 2018.
[3] M.P. Çetingul and C. Herman, "Quantification of the thermal signature of a melanoma lesion". *International Journal of Thermal Sciences*, vol. 50, n. 4, pp. 421–431, 2011.
[4] W.H. Clark, L. From, E.A. Bernardino and M.C. Mihm, "The histogenesis and biologic behavior of primary human malignant melanomas of the skin". *Cancer Research*, vol. 29, n. 3, pp. 705–727, 1969.
[5] A.A. Marghoob, K. Koenig, F.V. Bittencourt, A.W. Kopf and R.S. Bart, "Breslow thickness and Clark level in melanoma: support for including level in pathology reports and in American Joint Committee on Cancer staging". *Cancer*, vol. 88, n. 3, pp. 589–595, 2000.
[6] T.Y. Cheng and C. Herman, "Analysis of skin cooling for quantitative dynamic infrared imaging of near-surface lesions". *International Journal of Thermal Sciences*, vol. 86, pp. 175–188, 2014.
[7] A. Amri, S.H. Pulko and A.J. Wilkinson, "Potentialities of steady-state and transient thermography in breast tumour depth detection: A numerical study". *Computer Methods and Programs in Biomedicine*, vol. 123, pp. 68–80, 2016.
[8] M. Stücker, I. Horstmann, C. Nütchel, A. Röchling, K. Hoffmann and P. Altmeyer, "Blood flow compared in benign melanocytic naevi, malignant melanomas and basal cell carcinomas". *Clinical and Experimental Dermatology*, vol. 24, n. 2, pp. 107–111, 1999.
[9] M.P. Çetingul and C. Herman, "A heat transfer model of skin tissue for detection of lesions: Sensitivity analysis". *Physics in Medicine and Biology*, vol. 55, pp. 5933–5951, 2010.
[10] A. Breslow, "Thickness, cross-sectional areas and depth of invasion in the prognosis of cutaneous melanoma". *Annals of Surgery*, vol. 172, n. 5, pp. 902–908, 1970.
[11] J. Iljaž, L.C. Wrobel, M. Hriberšek and J. Marn, "Subdomain BEM formulations for the solution of bioheat problems in biological tissue with melanoma lesions". *Engineering Analysis with Boundary Elements*, vol. 83, pp. 25–42, 2017.
[12] J. Iljaž, L.C. Wrobel, M. Hriberšek and J. Marn, "Numerical modelling of skin tumour tissue with temperature-dependent properties for dynamic thermography". *Computers in Biology and Medicine*, vol. 112, article n. 103376, 2019.
[13] H.H. Pennes, "Analysis of tissue and arterial blood temperatures in the resting human forearm". *Journal of Applied Physiology*, vol. 1, n. 2, pp. 93–122, 1948.
[14] D. Fiala, G. Havenith, P. Brode, B. Kampmann and G. Jendritzky, "UTCI-Fiala multi-node model of human heat transfer and temperature regulation". *International Journal of Biometeorology*, vol. 56, n. 3, pp. 425–441, 2012.
[15] A.B.C. Silva, J. Laszczyk, L.C. Wrobel, F.L. Ribeiro and A.J. Nowak, "A thermoregulation model for hypothermic treatment of neonates". *Medical Engineering & Physics*, vol. 38, n. 9, pp. 988–998, 2016.
[16] A. Bhowmik and R. Repaka, "Estimation of growth features and thermophysical properties of melanoma within 3-D human skin using genetic algorithm and simulated annealing". *International Journal of Heat and Mass Transfer*, vol. 98, pp. 81–95, 2016.
[17] J. Iljaž, L.C. Wrobel, M. Hriberšek and J. Marn, "Solving inverse bioheat problems of skin tumour identification by dynamic thermography". *Inverse Problems*, vol. 36, article n. 035002, 2020.